Journal of
Materials Chemistry B

Accepted Manuscript

This article can be cited before page numbers have been issued, to do this please use: M. Gao, R. Wang, F. Yu, B. Li and L. Chen, *J. Mater. Chem. B*, 2018, DOI: 10.1039/C8TB01794H.

ROYAL SOCIETY OF CHEMISTRY

rsc.li/materials-b

View Article Online
DOI: 10.1039/C8TB01794H

Journal Name

ARTICLE

Imaging of intracellular sulfane sulfur expression changes under hypoxia stress via a selenium-containing near-infrared fluorescent probe

Received 00th January 20xx,
Accepted 00th January 20xx

DOI: 10.1039/x0xx00000x

www.rsc.org/

Min Gao,[†a,c] Rui Wang,[†a,b] Fabiao Yu,[a,b]* Bowei Li[a] and Lingxin Chen[a,d]*

Hypoxia is a significant global issue affecting the health of organism. Homeostasis of oxygen is critical for mammalian cell survival and cellular activities. Hypoxia stress can lead to cell injury and death, which attributes to many diseases. Sulfane sulfur is involved in many crucial roles of physiological processes via maintaining intracellular redox state and ameliorating oxidative damage. Therefore, real-time imaging of sulfane sulfur changes is important for understanding their biofunction in cells. In this work, we develop a new near-infrared (NIR) fluorescent probe BD-*di*SeH for imaging of sulfane sulfur changes in cells and *in vivo* under hypoxia stress. The probe includes two moieties: the NIR *azo*-BODIPY fluorophore equipped with a strong nucleophilic phenylselenol group (-SeH). The probe is capable for tracing the dynamic changes of endogenous sulfane sulfur based on a fast and spontaneous intramolecular cyclization reaction. The probe has been successfully used for imaging sulfane sulfur in *3D*-multicellular spheroid and in mice hippocampus under hypoxia stress. The overall levels of sulfane sulfur are affected by the degree and time of hypoxia stress. The results reveal a close relationship between sulfane sulfur and hypoxia in living cells and *in vivo*, which is better understanding the physiological and pathological processes involved by sulfane sulfur. Moreover, to indicate the effects of environmental hypoxia on aquatic animals, this excellent probe has been applied for sulfane sulfur detection in hypoxic zebrafish.

Introduction

Hypoxia is now a global and pressing environmental problem, which leads to deleterious ecological effects, therefore, it has received increasing scientific attention. Due to the rapid industrialization and human population growth, its severity is likely to be exacerbated.[1-2] Since oxygen is necessary for supporting normal physiological activities and survival of general organisms, hypoxia can disrupt high sophisticated, programmed processes in normal histogenesis and organogenesis and ultimately threaten the survival and fitness of organisms.[3] In vitro and in vivo studies show that hypoxia stress can induce a normal physiological response to imbalance in oxygen supply, triggers the burst of reactive oxygen species (ROS) in cells, and finally induces cell apoptosis. To prevent these damages, cells own intricate antioxidant regulatory systems to balance redox homeostasis. Reactive sulfur species (RSS) are composed of sulfur-containing molecules in biological systems, which act as regulators of intracellular redox state and prevent apoptosis.[4-5] RSS include disulfide-*S*-oxides, sulfenic acids, and thiyl radicals, thiols, disulfide, hydrogen sulfide, persulfide, polysulfide and other inorganic sulfur derivatives. These species have attracted more and more attention in physiological research.[6-9] Therefore, trapping the changes of reactive species are helping for better understanding the effects of hypoxia on organisms.

Sulfane sulfur belongs to RSS, which contains a reactive sulfur atom with six valence electrons but no charge (represented as S^0).[10] Generally, biologically sulfane sulfur are presented as persulfides (RSSH), hydrogen polysulfides (H_2S_n, $n \geq 2$), polysulfides (R-S_n-R, $n \geq 3$) and protein-bound elemental sulfur (S_8). Sulfane sulfur also plays antioxidative roles in the process of carcinogenesis as well as the activity of immune cells by regulation of some enzymes.[11-12] Moreover, H_2S and sulfane sulfur plays a redox partnership and coexist in biological systems. From this reactivity point-of-view, sulfane sulfur seems much more effective than H_2S in protein *S*-sulfhydration. Accumulating evidences indicate that the actual signaling molecules may be sulfane sulfur rather than H_2S. Currently few methods have been developed for sulfane sulfur detection due to their highly reactive and labile chemical properties. It is difficult to extract sulfane sulfur from living cells in real-time. As known, thiosulfoxide tautomers throughout exist with sulfane sulfur (Scheme 2). The most popular spectrophotometric assay for sulfane sulfur detection depend on the nucleophilic reaction with cyanide ions to generate thiocyanate which coordinates with Fe^{3+} yielding a red complex.[13] Unfortunately, this method needs complex processing

[a] CAS Key Laboratory of Coastal Environmental Processes and Ecological Remediation, Yantai Institute of Coastal Zone Research, Chinese Academy of Sciences, Yantai 264003, China. *E-mail: lxchen@yic.ac.cn.
[b] Institute of Functional Materials and Molecular Imaging, College of Emergency and Trauma, Hainan Medical University, Haikou, 571199, China. *E-mail: fbyu@yic.ac.cn.
[c] University of Chinese Academy of Sciences, Beijing 100049, China.
[d] College of Chemistry and Chemical Engineering, Qufu Normal University, Qufu 273165, China.
† These authors contributed equally.
Electronic Supplementary Information (ESI) available: [chemical synthesis and characterization of compounds, supplementary experiments, and data]. See DOI: 10.1039/x0xx00000x

View Article Online
DOI: 10.1039/C8TB01794H

of biological samples, which cannot meet the requirements for the real time and *in situ* detection. Therefore, it has huge challenge to accurately quantify trace amounts of sulfane sulfur in living cells and *in vivo*.

Fluorescence imaging exhibits various excellences for intracellular reactive species detection, which provides greater sensitivity, excellent selectivity, more convenience, less invasiveness as well as real-time imaging.[7,14-18] Despite the rapid progress in the development of fluorescent probes for biothiols detection, such as H_2S and glutathione,[7,19-22] fluorescent probes for sulfane sulfur detection in cells are still needed to be developed.[23-27] A majority of fluorescent probes were reported for the sensitive and selective detection of H_2S_n which belongs to sulfane sulfur.[28-38] Among them, Xian's group reports a series of fluorescent probes based on the nucleophilic property of H_2S_n. Our group further proposes two fluorescent probes for the crosstalk research between H_2S_n and superoxide anion.[28,33] Moreover, we investigates another species of sulfane sulfur, cysteine hydropersulfide (Cys-SSH), in living cells and *in vivo* based on a ratiometric NIR fluorescent probe.[39] We suppose that the overall levels of intracellular sulfane sulfur will associate with various of physiological and pathological processes. Unfortunately, few fluorescent probes were designed for sulfane sulfur detection.[25] Moreover, of particular interest are fluorescent probes that emit in the near-infrared (NIR) region, whereas biological autofluorescence minimally so as to allow tissue penetration for several centimeters.[40-43] Therefore, we strive to develop a fluorescent probe that features NIR absorption and emission for the overall levels of sulfane sulfur detection in cells and *in vivo*.

Herein, we designed a NIR fluorescent probe BD-*di*SeH, which integrated 2-hydroselenobenzoate fragment to NIR *azo*-BODIPY fluorophore, for the detection of sulfane sulfur in living cells and *in vivo* under hypoxic condition. BD-*di*SeH exhibited excellent selectivity and high sensitivity for the detection of sulfane sulfur. The relationship between the changes of sulfane sulfur and the degree and time of hypoxia stress had been investigated in cells, in 3D-multicellular spheroid, in hippocampus and *in vivo*, which clearly elucidated that changes of sulfane sulfur under hypoxic condition for investigating the physiological and pathological processes mediated by sulfane sulfur.

Experimental

Synthesis and characterization of BD-*di*SeH. 2,2'-diselanediyldibenzoic acid (80.03 mg, 0.2 mmol) and aza-BODIPY (53.0 mg, 0.1 mmol), 1-ethyl-3-(3-dimethylaminopropyl)carbodiimide hydrochloride (EDC, 38.4 mg, 0.2 mmol) and 4-dimethylaminopyridine (DMAP, 2.44 mg, 0.02 mmol) in CH_2Cl_2 (50 mL) were stirred for 12 hours at 25 °C. Then the mixture was neutralized with dilute HBr and extracted with CH_2Cl_2. Then, the organic phase was separated and evaporated to dryness and the resulting residue was subjected to column chromatography and eluted with CH_2Cl_2 for purification. The product (64.8 mg, 0.05 mmol) and sodium borohydride (37.8 mg, 1 mmol) were reacted for 6 h in ethanol (30 mL) under Ar atmosphere at 25 °C. And then the mixture was partitioned between CH_2Cl_2 and H_2O. The organic layer was separated and dried over Na_2SO_4. The crude product of BD-*di*SeH was purified by column chromatography (eluted with CH_2Cl_2). The product was obtained as dark green crystals. Yield: 37.4 mg, 41.7%. ^{1}H NMR (500 MHz, $CDCl_3$-D_1) δ (ppm): 8.16-8.14 (m, 8H), 8.08-8.07 (m, 5H), 7.52-7.43 (m, 11H), 7.38-7.36 (m, 4H), 1.26 (s, 2H). ^{13}C NMR (125 MHz, $CDCl_3$-D_1) δ (ppm): 163.88, 161.33, 158.49, 152.82, 145.70, 144.40, 141.41, 140.41, 132.20, 131.89, 131.63, 131.21, 131.18, 131.15, 129.67, 129.43, 129.39, 129.32, 129.07, 128.69, 127.75, 127.10, 121.94, 119.11. LC-MS (ESI$^-$): $C_{46}H_{30}BF_2N_3O_4Se_2$ calcd. 897.0628, found [M + K$^+$] 934.0129.

Scheme 1. Synthesis Route for BD-*di*SeH

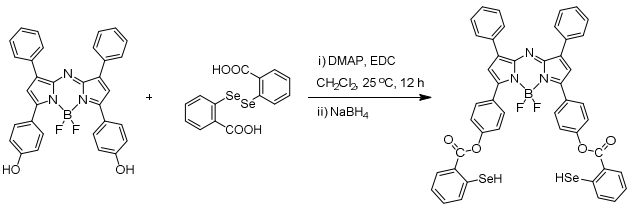

Cell culture and confocal imaging. Human neuroblastoma (SH-Sy5y) cells, mouse macrophage (RAW 264.7) cells, human lung carcinoma (A549) cells, human cervical carcinoma (Hela) cells , Human embryonic kidney 293 (HEK 293) cells, human hepatocellular liver carcinoma (HepG2) cells, human hepatocellular liver carcinoma (SMMC7721) cells were obtained from the cell bank of the Shanghai Institute of Biochemistry and Cell Biology (Shanghai, China). A549 cells, RAW 264.7 cells, SMMC7721 cells, SH-Sy5y cells were cultured in RPMI 1640 medium supplemented with 10% fetal bovine serum (FBS) at 37 °C in a humidified atmosphere containing 5% CO_2. Hela cells and HepG2 cells were cultured in DMEM medium supplemented with 10% FBS at 37 °C in a humidified atmosphere containing 5% CO_2. HEK 293 cells were cultured in MEM medium supplemented with 10% fetal bovine serum (FBS) at 37 °C in a humidified atmosphere containing 5% CO_2. Fluorescent images were acquired on an Olympus FluoView FV1000 confocal laser-scanning microscope (Japan) with an objective lens (×60). The excitation wavelength was 635 nm. Cell imaging was carried out after being washed with PBS for three times.

Hypoxic conditions in cell incubation. 0.1% O_2 concentration was generated with an AnaeroPack™ (Mitsubishi Gas Chemical Campany, Co. Inc., Japan). 1 ~ 20% O_2 concentration was generated with a multi gas incubator (Sanyo) by means of N_2 substitution.

Formation of SH-SY5Y multicellular spheroids. SH-SY5Y multicellular spheroids (MCs) were cultured in low attachment multiwell plates (Corning® Costar® Ultra). The MCs with the diameter of 300 - 400 nm were picked and incubated with BD-*di*SeH (1 μM) for 8 h at 37 °C. Then the MCs were washed with PBS and observed with confocal laser scanning microscopy.

View Article Online
DOI: 10.1039/C8TB01794H

Results and discussion

Design strategy for probe BD-*di*SeH. It seems that a NIR fluorescent probe can accept the challenge of rapid and sensitive detection of sulfane sulfur in living cells and *in vivo*. To achieve our design strategy, BODIPY platform was particularly selected as fluorophore due to its high molar absorption coefficients and fluorescence quantum yields.[44] Sulfane sulfur is reactive and labile, and commonly associated with their thiosulfoxide tautomers. This chemical property will provide a highly reactive site that a sulfur atom in thiosulfoxide can be readily removed by a nucleophilic group such as CN^- (Scheme 2). With this inspiration, we suggested that the selenol group (–SeH) in phenylselenol (pKa 5.9) should be a better nucleophilic group than the mercapto group (–SH) in thiophenol (pKa 6.5).[25] The strong nucleophilicity of –SeH would be benefit for the selectivity, sensitivity, and kinetics of probe for sulfane sulfur detection.[45] The probe BD-*di*SeH was devised by incorporating two sulfane sulfur responsive trigger 2-hydroselenobenzoate containing –SeH sub-moiety into BODIPY platform via an ester bridge (Scheme 2). In the presence of sulfane sulfur, the –SeH group captured a sulfur atom in thiosulfoxide affording a reactive intermediate (BD-*di*SeSH), followed by an intramolecular nucleophilic attack on the ester bridge. Finally, the fluorophore released. The detailed synthetic protocols are displayed in Scheme 1.

Scheme 2. Design strategy and proposed detection mechanism of BD-diSeH towards sulfane sulfur.

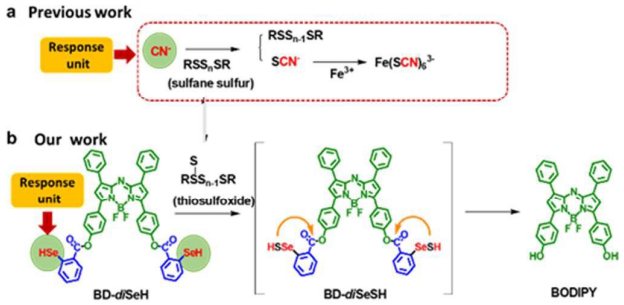

Spectral properties of probe BD-diSeH. To demonstrate the efficiency of BD-*di*SeH for measuring sulfane sulfur, the absorption and fluorescence spectra of BD-*di*SeH (10 μM) were examined under simulated physiological conditions (10 mM HEPES, pH 7.4, 20 % fetal bovine serum). As shown in Fig. 1a, BD-*di*SeH exhibited an absorption peak centered at 702 nm ($\varepsilon_{702\ nm} = 2.98\times10^5\ cm^{-1}M^{-1}$). The quantum yields of BD-*di*SeH was determined to 0.002. After reaction with Na_2S_4 as the model source of sulfane sulfur for the following tests, a new absorption peak appeared at 707 nm ($\varepsilon_{707\ nm} = 3.74\times10^5\ cm^{-1}M^{-1}$), which indicated that BD-*di*SeH reacted with sulfane sulfur and released the fluorophore. Upon addition of different concentration of Na_2S_4 (0 - 20 μM) to the buffer solution containing 10 μM BD-*di*SeH, the fluorescence intensity was gradually increased accompanied with the increasing concentrations of sulfane sulfur in the NIR region (Fig. 1b). The fluorescence intensity at 737 nm was linearly related to the concentration of sulfane sulfur within the given range (Fig. 1c). The regression equation was $F_{\lambda ex/em\ (707/737\ nm)} = 3.32 \times 10^5 [Na_2S_4] + 4.59 \times 10^3$ with r = 0.9936. The limit of detection was determined to be 2.3 nM ($3\sigma/\kappa$) under the testing experimental conditions, which indicated that the probe had a high sensitivity for the detection of sulfane sulfur. To verify whether the probe was suitable for the physiological detection, the pH effect on the probe was investigated. These results indicated that BD-*di*SeH could work effectively at pH 7.4 (Fig. S1). Now that our probe could detect sulfane sulfur quantitatively under simulated physiological conditions, we next directly tested the concentration of sulfane sulfur in BALB/c mice serum using BD-*di*SeH (10 μM). The concentration of sulfane sulfur in mice serum could reach at 12.4 ± 2.5 μM (the red point in Fig. 1c). The results demonstrated that our probe could qualitatively and quantitatively detect sulfane sulfur in biological samples.

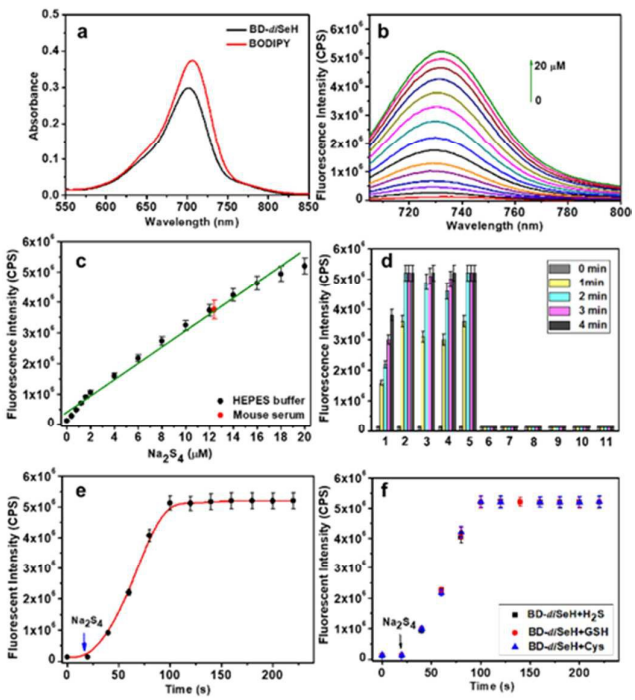

Fig. 1. (a) UV-vis absorption spectra of BD-*di*SeH (10 μM) before and after treatment of Na_2S_4 (20 μM). (b) Fluorescence spectra of BD-*di*SeH (10 μM) upon addition of Na_2S_4 (0-20 μM). Spectra were obtained after incubation of the probe with Na_2S_4 for 5 min. (c) The corresponding linear relationship between fluorescent intensity and Na_2S_4 concentration (0-20 μM) in buffer solution. The red point was the mean fluorescent intensity of mice serum. (d) Time-dependent enhancement in fluorescence response of BD-*di*SeH (10 μM) toward various RSS. 1. Na_2S_2 20 μM; 2. Na_2S_4 20 μM; 3. $PhCH_2S_4CH_2Ph$ 20 μM; 4. Cys-Poly-Sulfide 20 μM; 5. S_8 20 μM; 6. NaHS 100 μM, 7. GSH 1 mM, 8. Cys 500 μM, 9. Hcys 500 μM, 10. Cys-Cys 500 μM, 11. GSSG 500 μM. Bars represent fluorescent intensity during 0, 1, 2, 3, and 4 min after addition of various RSS. (e) Time-dependent fluorescence changes of BD-*di*SeH upon addition of Na_2S_4 (20 μM). (f) Time-dependent fluorescence changes of BD-*di*SeH upon addition of Na_2S_4 (20 μM) in the presence of interfering thiols H_2S, GSH and Cys (1 mM). All spectra were acquired in 10 mM HEPES (20% fetal bovine serum, v/v, pH 7.4). $\lambda_{ex/em}$= 707/737 nm.

View Article Online
DOI: 10.1039/C8TB01794H

Selectivity. Fluorescent probe must offer rapid and selective response to sulfane sulfur because sulfane sulfur undergo rapid metabolism in biological systems. Selectivity and response time of BD-*di*SeH (10 μM) towards sulfane sulfur over other RSS were checked in 10 mM HEPES (pH 7.4, 20% fetal bovine serum, v/v). As shown in Fig. 1d, five representative sulfane sulfur including Na_2S_2, Na_2S_4, dibenzyl oligosulfane ($PhCH_2S_4CH_2Ph$), cysteine polysulfide and elemental sulfur (S_8) were selected as testing models. Once triggered by these sulfane sulfur, BD-*di*SeH offered obvious fluorescence increase within 1 min. In contrast, no fluorescence response was obtained towards other RSS even under much higher concentration within 4 min, such as NaHS (100 μM), glutathione (GSH, 1 mM), cysteine (Cys, 500 μM), homocysteine (Hcys, 500 μM), cystine (Cys-Cys, 500 μM) and oxidized glutathione (GS-GS, 500 μM). Moreover, the reaction of probe BD-*di*SeH (10 μM) with Na_2S_4 (20 μM) at 37 °C yielded a time-dependent plot. The saturation of fluorescence intensity was obtained after incubation of Na_2S_4 for 80 s with a 40-fold fluorescence increase (Fig. 1e). In addition, the probe showed high selectivity for sulfane sulfur even coexisted with main biothiols at physiological concentrations (Fig. 1f). All these results demonstrated that BD-*di*SeH had high selectivity and rapid response for sulfane sulfur.

MTT assay and photostability. The above successful results inspired us to apply our new fluorescent probe in biological systems. Before imaging sulfane sulfur in living cells, the cytotoxicity of BD-*di*SeH was tested in A549 cells via MTT assay. As shown in Fig. S2, almost 90% cells were survived after incubated with 5 μM BD-*di*SeH for 24 h. The cell viability maintained at 85% after treated with 10 μM BD-*di*SeH. The result indicated that BD-*di*SeH would exhibit low cytotoxicity to cells. The photostability of BD-*di*SeH was also investigated through a time-dependent fluorescence measurement. The stable fluorescence intensity indicated the probe BD-*di*SeH could be used for long-time cells imaging (Fig. S3).

Imaging exogenous and endogenous sulfane sulfur in cells.

The probe BD-*di*SeH was then applied for the detection of exogenous and endogenous sulfane sulfur in living cells. Cells in Figure 2 were cultured with BD-*di*SeH for 15 min at 37 °C before image acquisition. A549 cells in Figure 2a showed weak intracellular fluorescence. N-ethylmaleimide (NEM) can scavange the intracellular endogenous RSS. Cells in Figure 2b which pretreated with NEM exhibited nearly no fluorescence signal in these cells (Figure 2b). The result illustrated that BD-*di*SeH could be used to detect endogenous sulfane sulfur in cells. The next group were treated with Na_2S_4 (1 μM) for 15 min. A strong fluorescence in the cells was obtained (Figure 2c). Our probe could detect exogenous sulfane sulfur in living cells. The following additional studies were performed to verify whether our probe could be used to imaging sulfane sulfur which were generated by the enzymes cystathionine γ-lyase (CSE) and 3-mercaptopyruvate sulfurtransferase (3-MST) in cells.[46] Intracellular CSE mRNA was overexpressed upon stimulation of lipopolysaccharide (LPS). N-acetyl-L-cysteine (NAC) was utilized to stimulate the activity of 3-MST and to elevate the level of sulfane sulfur.[47,48] After exposing the cells in Figure 2d with LPS for 16 h, there existed an increasing fluorescence intensity. The other cells were incubated with NAC for 48 h, a strong fluorescence response was acquired (Figure 2e). As control experiments, the cells were pretreated with a CSE inhibitor, DL-propargylglycine (PAG, 1 mM) and 3-MST inhibitor, α-ketoglutarate (6 mM), respectively (Figure 2f and 2g).[49] Then, cells were treated as described in Figure 2d and 1e. The fluorescence intensity of the cells was significantly reduced. These results demonstrated that the probe BD-*di*SeH was used for imaging of sulfane sulfur that generated by enzyme CSE and 3-MST.

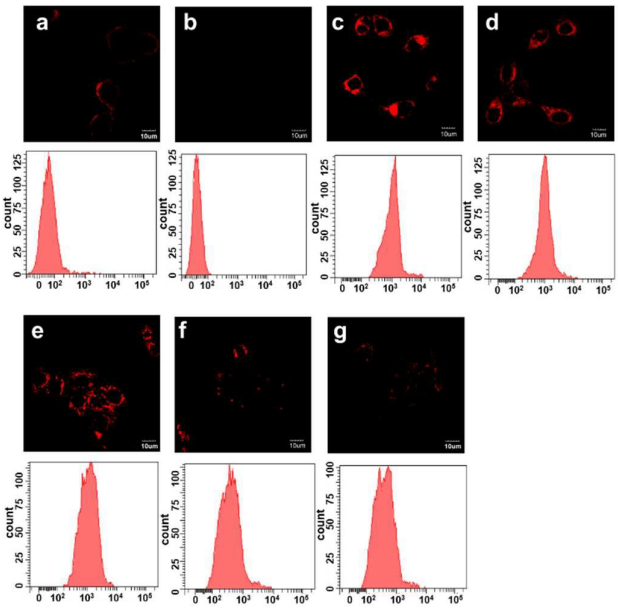

Fig. 2. Confocal microscopy images and flow cytometry analysis of A549 cells for the detection of sulfane sulfur using BD-*di*SeH. All the cells were stained with BD-*di*SeH (1 μM) for 15 min and then imaging. (a) A549 cells were treated with BD-*di*SeH for 15 min at 37 °C; (b) Cells incubated with 5 mM NEM for 30 min; (c) The cells were incubated with Na_2S_4 (1 μM) for 15 min at 37 °C; (d) A549 cells preincubated with LPS (1 μg/mL) for 16 h at 37 °C; (e) A549 cells preincubated with NAC (0.5 mM) for 48 h at 37 °C; (f) The cells were preincubated with DL-propargylglycine (PAG, 1 mM), then treated with LPS (1 μg/mL) for 16 h at 37 °C; (g) The cells were pretreated with a-ketoglutarate (6 mM), then treated with NAC (0.5 mM) for 48 h at 37 °C. Fluorescence collection windows constructed from 680 to 780 nm for BD-*di*SeH. λ_{ex} = 635 nm.

We then explored the levels of sulfane sulfur in different cell lines. Human neuroblastoma (SH-SY5Y) cells, mouse macrophage 264.7 (RAW 264.7) cells, human cervical carcinoma (Hela) cells, human embryonic kidney 293 (HEK 293) cells, human hepatocellular liver carcinoma (HepG2) cells, and human hepatocellular liver carcinoma (SMMC7721) cells were employed to perform the tests. The cells were firstly incubated with BD-*di*SeH (1 μM) for 15 min. Weak fluorescent intensities were observed in Fig. S4a - f. The results suggested that different cell lines held different concentrations of sulfane sulfur. After washed with PBS and further treated with Na_2S_4 (1 μM) for another 15 min, as expected, strong fluorescence were observed in these cells indicating that BD-*di*SeH could be employed to detect sulfane sulfur in different cell lines.

View Article Online
DOI: 10.1039/C8TB01794H

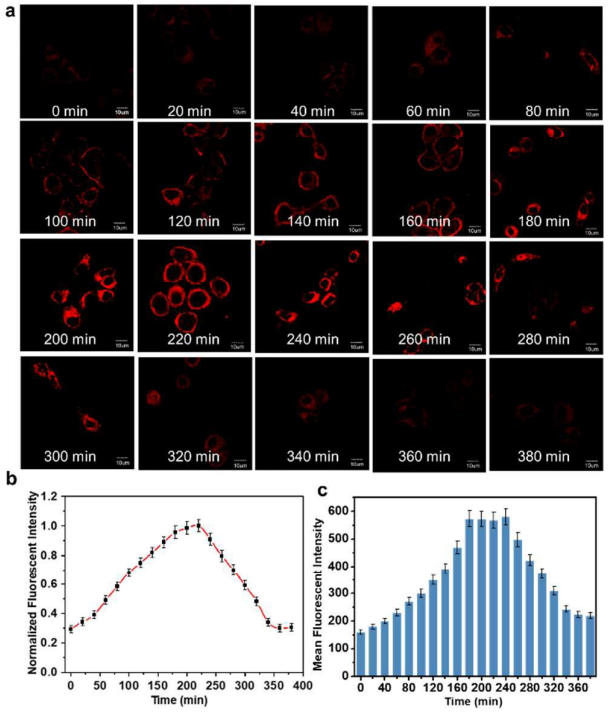

Fig. 3. (a) Fluorescence images of A549 cells using BD-*di*SeH at different time points of hypoxic condition. (b) Normalized fluorescent intensity of single cell in Fig. 3a (n = 8). (c) Mean fluorescent intensity of flow cytometry analysis for Fig. 3a. A549 cells were pre-incubated with BD-*di*SeH (1 μM) and then putted in an AnaeroPack. Fluorescence collection windows constructed from 680 to 780 nm for BD-*di*SeH. λ_{ex} = 635 nm.

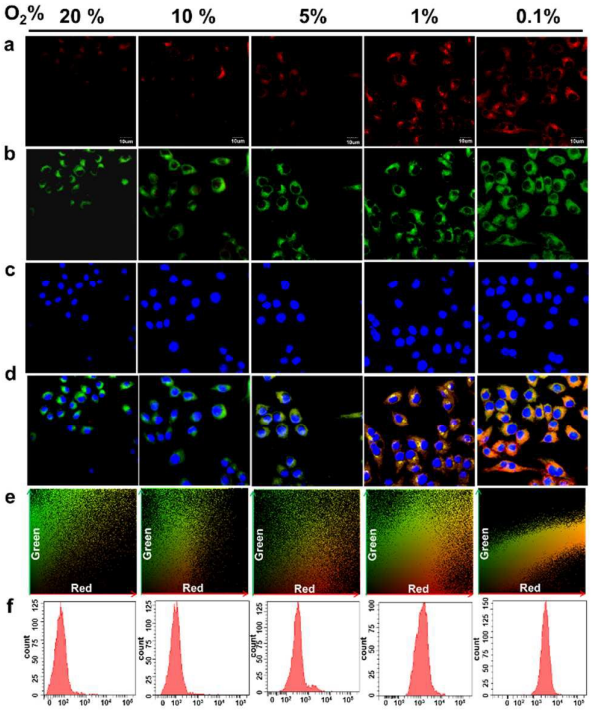

Fig. 4. Fluorescence images of A549 cells using BD-*di*SeH at different level of oxygen concentration (20%, 10%, 5%, 1%, 0.1%). A549 cells were incubated with BD-*di*SeH (1 μM) for 3 h under various oxygen concentrations (a). Then the cells were further incubated with Calcein-AM (5 μM, b), and Hoechst 33342 (1 μg/mL, c) for 30 min. (d) Colocalization images of the red, green and blue channels. (e) Correlation plot of the red and green channels. (f) Flow cytometry assay of A549 cells using BD-*di*SeH at different level of oxygen concentration (20%, 10%, 5%, 1%, 0.1%). Fluorescence collection windows constructed from 680 to 780 nm for BD-*di*SeH, from 500 to 550 nm for Calcein-AM, from 425 to 500 nm for Hoechst 33342, λ_{ex} = 635, 488, and 405 nm, respectively.

Influence on sulfane sulfur under hypoxia stress. Sulfane sulfur exhibits protective properties by scavenging free radicals and enhancing the activities of antioxidative enzymes such as: glutathione peroxidase, glutathione reductase, as well as superoxide dismutase.[50-52] As known, hypoxia stress can cause the overproduction of oxygen radicals and lipid peroxides which will inhibit the activity of antioxidant enzymes. Therefore, we attempted to trace the dynamic changes of sulfane sulfur with BD-*di*SeH in living cells under hypoxic condition. One assay was performed to examine the generation of sulfane sulfur under hypoxic condition at different time points using AnaeroPack (<0.1% O_2, 5% CO_2). There existed a time-dependent increase in fluorescence intensity in A549 cells from 0 min to 180 min, and a decrease in fluorescent intensity was observed in cells from 240 min to 380 min. However, during the time interval of 180 min to 240 min, the fluorescent intensity was saturated and maintained (Fig. 3a and 3b). Flow cytometry studies were well consistent with imaging assays (Fig. 3c). The level changes of sulfane sulfur could be attributed to self-protection of biological system. The results indicated that our probe could work well in tracing dynamic endogenous sulfane sulfur changes under hypoxic stress.

Another assay was carried out to evaluate the production of sulfane sulfur under various oxygen concentrations. The probe BD-*di*SeH was loaded into A549 cells and incubated under various oxygen concentrations (20%, 10%, 5%, 1%, 0.1%) for 3 h, respectively. As shown in Fig. 4, the fluorescent intensity was increased according to the decreased concentrations of oxygen. There was a strong increase in fluorescent intensity when the oxygen concentration is less than 1%. Flow cytometry studies were performed to further confirm these results. The result displayed that the fluorescent intensities of the cells was related to the degrees of hypoxic stress. These new generation of sulfane sulfur could play a role in protecting cells from oxidative damage induced by hypoxic stress.

In addition, subcellular location of BD-*di*SeH in A549 cells were investigated by co-staining with cytoplasm targetable dye, Calcein-AM (5 μM, Green channel) and a nucleus fluorescence marker, Hochest 33342 (1 μg/mL, Blue channel). The images merged well between BD-*di*SeH and Calcein-AM (Fig. 4 Overlay) indicating a preferential distribution of BD-*di*SeH in cytoplasm.Moreover, the color–pair intensity correlation analysis showed that high correlated plot between the intensity distribution of BD-*di*SeH and Calcein-AM.

View Article Online
DOI: 10.1039/C8TB01794H

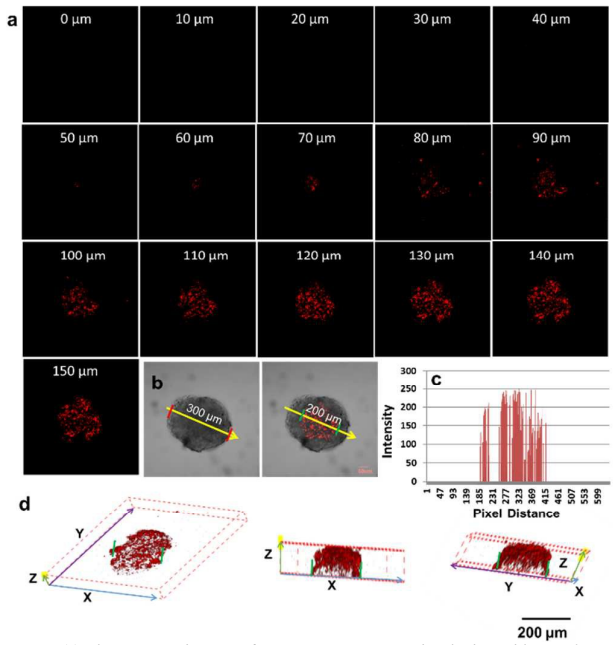

Fig. 5. (a) Fluorescence images of SH-SY5Y MCs upon incubation with BD-*di*SeH (1 μM) for 8 h at 37 ℃. The images were acquired by Z-stack scan at 10 μm intervals. Fluorescence collection window was constructed from 680-780 nm. (b) Bright field image and overlay image. (c) The quantitative and spatial distribution of fluorescence signal intensity of the yellow arrow in Fig. 5b. (d) Different angles of MCs by Z-stack scan images reconstruction.

Imaging sulfane sulfur in 3D-multicellular spheroid. Having assessed the levels of sulfane sulfur in monolayer cells, we next attempted to evaluate the levels of sulfane sulfur in three-dimensional multicellular spheroid (3D-MCs) which were cultured in a nonadhesive environment. We proposed that the inside of 3D-MCs prohibited oxygen from outside forming a hypoxic environment in its interior. SH-SY5Y cells with diameter of 300 μm (Fig. 5) were selected to construct 3D-MCs model. After treated with BD-*di*SeH for 8 h under 20% O_2, 3D-MCs exhibited intense fluorescence emission only in its interior (*z*-axis: 50 – 150 μm), while the signal was quite weak in the periphery (*z*-axis: 0 – 50 μm). The images of Z-stack reconstruction for 3D-MCs exhibited the fluorescence signals was activated at a depth of 150 μm, which indicated that the BD-*di*SeH could penetrate the interior for sulfane sulfur imaging (Fig. 5a). The 3D perspective images further verified that the fluorescence emitted from the interior instead of external part (Fig. 5d). The quantitative and spatial distribution of fluorescence signal intensity of the yellow arrow in Fig. 5b was shown in Fig. 5c. The result indicated that the hypoxic interior of 3D-MCs induced the overproduction of sulfane sulfur. Our probe was ready for the detection of sulfane sulfur changes in hypoxic model.

Imaging sulfane sulfur in hypoxic brain. The brain occupies approximately 2% - 3% of the body's weight while it consumes approximately 20% of the body's oxygen. Therefore, it is very sensitive to hypoxia. Cerebral hypoxia will lead to neurologic dysfunction manifest, and ultimately cause brain injury, such as ischemic stroke[53] and Alzheimer's disease.[54] Brain possesses high sulfane sulfur level to confront the overproduction of hypoxia-induced ROS. We strived to explore the concentration changes of sulfane sulfur during cerebral hypoxia. BALB/C mice were placed in normobaric hypoxic chambers for 1 - 4 days to build hypoxic mouse models (Fraction of inspiration O_2, FIO2 11%). After carefully isolated the hippocampus from the sacrificed mice, the hippocampus slices were stained with BD-*di*SeH for 20 min. The above experiments were all performed in an anoxic glove box (11% O_2). As shown in Fig. 6a, an obvious decrease in fluorescent intensity (1 – 3 days) was observed over hypoxic time indicating that the levels of sulfane sulfur reduced in the hippocampus (Fig. 6b). The results implied that the hypoxia-induced ROS in the hippocampus should deplete most of sulfane sulfur. However, we found that the body began its self-repair mechanism to increase the level of sulfane sulfur in the 4th day. Hypoxia-inducible factor 1α (HIF-1α) is involved in response to low oxygen concentration in the cellular milieu. It is expressed under hypoxia. The expression of HIF-1α was positively correlated with the hypoxic time (Fig. 6c). These results indicated that our probe could be applied for sulfane sulfur imaging in the hippocampus under hypoxic condition, which could better clarify the level changes of sulfane sulfur during hypoxic period.

Imaging sulfane sulfur in mice. Near-infrared fluorescence is facilitative for the deep imaging in organisms. To explore the capability of BD-*di*SeH for sulfane sulfur detection in vivo, BALB/c mice were selected as testing models for *in vivo* imaging using an *In vivo* Imaging system. BALB/c mice in Figure 5d were divided into three groups. Mice in group a were injected intraperitoneally with BD-*di*SeH for 20 min as a control. However, in group b, the mice were firstly pretreated with Na_2S_4 (20 μM, 50 μL in saline), followed by incubation with BD-*di*SeH for 20 min. The mice exhibited strong fluorescence increase. In group c, the mice were given intraperitoneal (i.p.) cavity injection with LPS (10 μg/mL, 100 μL in 1:9 DMSO-saline, v/v) for 24 h to induce CSE mRNA overexpression.[55] As a CSE activator, pyridoxal-phosphate (PLP, 1 μM) was injected in i.p. cavity for improving the CSE activity to promote the initial production rate of sulfane sulfur. Then the mice were treated with BD-*di*SeH for 20 min prior to *in vivo* imaging. As expected, dramatic fluorescence emission was obtained in group c. The quantification of mean fluorescent intensities for each group were shown in Figure 5e. All results demonstrated that BD-*di*SeH could be applied to detect sulfane sulfur in living animals.

Imaging sulfane sulfur in hypoxic zebrafish. Hypoxia is a significant issue in aquatic systems. As a valuable vertebrate model organism, zebrafish have been used in a variety of biological research. We selected zebrafish as research object to investigate the effects of hypoxia on the expression of sulfane sulfur. The zebrafish were loaded with BD-*di*SeH for 15 min before imaging. As shown in Figure 6f, two-day-old zebrafish exhibited weak fluorescence signal. After loaded with Na_2S_4, the zebrafish gave a strong fluorescence signal (Figure 6g). The zebrafish treated under different oxygen levels from 20% to 5% for 1 h produced a gradual increase in fluorescence signal (Figure 6h). The expressions of sulfane sulfur in hypoxic

View Article Online
DOI: 10.1039/C8TB01794H

zebrafish were increased, which may be ascribed to the physiological response against hypoxia. The released sulfane sulfur was likely to inhibition of the hypoxia-induced ROS elevation. These results revealed that this probe was suitable for imaging sulfane sulfur *in vivo* under hypoxic condition.

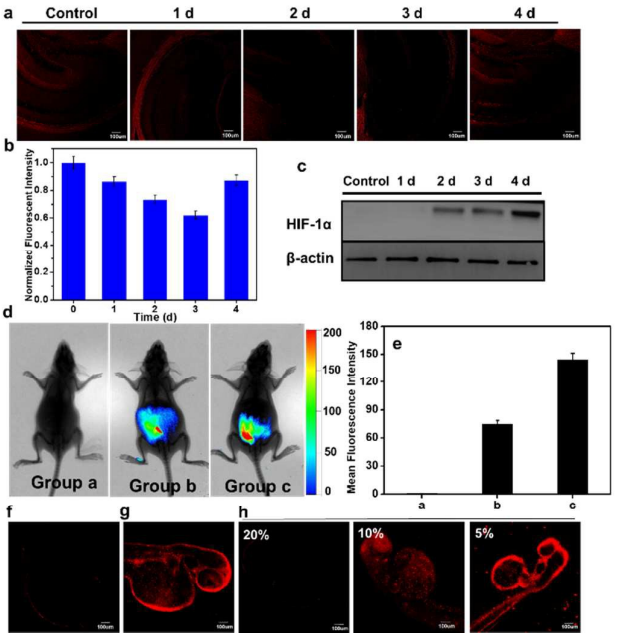

Fig. 6. (a) Confocal fluorescence images of hippocampus slice using BD-*di*SeH. The hippocampus slices were incubated with BD-*di*SeH (1 μM) for 20 min. λ_{ex} =635 nm. Fluorescence collection windows was constructed from 680-780 nm. (b) Normalized fluorescent intensity of Fig. 6a. Data are presented as means ± SD (n = 5). (c) Western blot analysis of HIF-1α. *β*-actin was taken as the loading control. (d) Fluorescence images of BALB/c mice visualizing sulfane sulfur level changes using BD-*di*SeH. Images displayed represent emission intensities collected window: 700−800 nm, λ_{ex} = 680 nm. Group a was injected i. p. with BD-diSeH (10 μM, 50 μL in 1:9 DMSO-saline, v/v) for 20 min. Group b was firstly pretreated with Na_2S_4 (20 μM, 50 μL in saline), then injected with BD-*di*SeH for 20 min. Group c was firstly injected with LPS (10 μg/mL, 100 μL in 1:9 DMSO-saline, v/v) for 24 h, and PLP (1 μM, 50 μL in saline) for 2 h, then injected with BD-*di*SeH for 20 min. (e) Mean fluorescent intensity of Group a−c. The total number of photons from the entire peritoneal cavity of the mice was integrated. Data are presented as means ± SD (n = 5). (f) Fluorescence images of zebrafish visualizing sulfane sulfur level changes using BD-*di*SeH. The zebrafish was treated with BD-*di*SeH (1 μM) for 15 min. (g) The zebrafish was preteated with Na_2S_4 (2 μM), then injected with BD-*di*SeH for 15 min. (h) Fluorescence images of zebrafish using BD-*di*SeH at different level of oxygen concentration. The zebrafish was incubated with BD-*di*SeH (1 μM) for 1 h under various oxygen concentrations (20%, 10%, 5%).

Conclusions

In summary, we have rationally designed and synthesized a fluorescent probe BD-*di*SeH which enables real-time imaging of endogenous and exogenous sulfane sulfur in living cells, in 3D-multicellular spheroid, in hippocampus, as well as *in vivo*. The probe BD-*di*SeH is composed of two moieties: the strong nucleophilic phenylselenol group (-SeH) is integrated into the NIR *azo*-BODIPY fluorophore via an ester bridge. BD-*di*SeH exhibits excellent selectivity and high sensitivity for the detection of sulfane sulfur. This new developed probe could serve as an effective imaging tool for tracing endogenous sulfane sulfur changes under hypoxia stress. The relationship between the changes of sulfane sulfur and the degree and time of hypoxia stress has been investigated in cells, in 3D-multicellular spheroid, and in hippocampus. The results presented here hold a great promise for exploring the biological and physiological roles of endogenous sulfane sulfur in living systems.

Conflicts of interest

There are no conflicts to declare.

Acknowledgements

We thank the National Nature Science Foundation of China (No. 21775162, No. 41776110, and No. 21575159), the program of Youth Innovation Promotion Association, CAS (Grant 2015170), State Key Laboratory of Environmental Chemistry and Ecotoxicology, Research Center for Eco-Environmental Sciences, CAS (Grant KF2016-22), and the Key Laboratory of Sensor Analysis of Tumor Marker Ministry of Education, Qingdao University of Science and Technology (Grant SATM201705).

Notes and references

1 R. M. Yu, D. L. Chu, T. F. Tan, V. W. Li, A. K. Chan, J. P. Giesy, S. H. Cheng, R. S. Wu and R. Y. Kong. Leptin-mediated modulation of steroidogenic gene expression in hypoxic zebrafish embryos: implications for the disruption of sex steroids. *Environ. Sci. Technol.* 2012, **46**, 9112-9119.

2 J. A. Fitzgerald, H. M. Jameson, V. H. Dewar Fowler, G. L. Bond, L. K. Bickley, T. M. Uren Webster, N. R. Bury, R. J. Wilson and E. M. Santos, Hypoxia suppressed copper toxicity during early development in zebrafish embryos in a process mediated by the activation of the HIF signaling pathway. *Environ. Sci. Technol.* 2016, **50**, 4502-4512.

3 E. H. Shang and R. S. Wu, Aquatic hypoxia is a teratogen and affects fish embryonic development. *Environ. Sci. Technol.* 2004, **38**, 4763-4767.

4 P. Nagyand and M. T. Ashby, Reactive sulfur species: Kinetics and mechanisms of the oxidation of cysteine by hypohalous acid to give cysteine sulfenic acid. *J. Am. Chem. Soc.,* 2007, **129** (45), 14082-14091.

5 G. I. Giles and C. Jacob, Reactive sulfur species: An emerging concept in oxidative stress. *Biol. Chem.,* 2002, **383** (3-4), 375-388.

6 M. C. H. Gruhlke and A. J. Slusarenko, The biology of reactive sulfur species (RSS). *Plant Physiol. Bioch.,* 2012, **59**, 98-107.

7 H. S. Jung, X. Chen, J. S. Kim and J. Yoon, Recent progress in luminescent and colorimetric chemosensors for detection of thiols. *Chem. Soc. Rev.,* 2013, **42** (14), 6019-6031.

8 X. Zhang, J. Yin and J. Yoon, Recent advances in development of chiral fluorescent and colorimetric sensors. *Chem. Rev.,* 2014, **114** (9), 4918-4959.

9 K. Ono, T. Akaike, T. Sawa, Y. Kumagai, D. A. Wink, D. J. Tantillo, A. J. Hobbs, P. Nagy, M. Xian, J. Lin and J. M. Fukuto, Redox chemistry and chemical biology of H_2S, hydropersulfides, and derived species: Implications of their possible biological activity and utility. *Free Radical Biol. Med.,* 2014, **77**, 82-94.

View Article Online
DOI: 10.1039/C8TB01794H

10 J. I. Toohey and A. J. L. Cooper, Thiosulfoxide (sulfane) sulfur: new chemistry and new regulatory roles in biology. *Molecules,* 2014, **19** (8), 12789-12813.
11 G. Roos and J. Messens, Protein sulfenic acid formation: From cellular damage to redox regulation. *Free Radical Biol. Med.,* 2011, **51** (2), 314-326.
12 S. Laxman, B. M. Sutter, X. Wu, S. Kumar, X. Guo, D. C. Trudgian, H. Mirzaei and B. P. Tu, Sulfur amino acids regulate translational capacity and metabolic homeostasis through modulation of tRNA thiolation. *Cell,* 2013, **154** (2), 416-429.
13 J. L. Wood, Sulfane sulfur. *Methods in Enzymology,* 1987, **143**, 25-29.
14 T. Ueno and T. Nagano, Fluorescent probes for sensing and imaging. *Nat. Methods,* 2011, **8** (8), 642-645.
15 X. Li, X. Gao, W. Shi and H. Ma, Design strategies for water-soluble small molecular chromogenic and fluorogenic probes. *Chem. Rev.,* 2014, **114** (1), 590-659.
16 H. Liu, K. Li, X. Hu, L. Zhu, Q. Rong, Y. Liu; X. Zhang, J. Hasserodt, F. Qu and W. Tan, In situ localization of enzyme activity in live cells by a molecular probe releasing a precipitating fluorochrome, *Angew. Chem. Int. Ed.*, 2017, **56**, 11788-11792.
17 H. Liu, Y. Liu, P. Wang and X. Zhang, Molecular engineering of two-photon fluorescent probes for bioimaging applications, *Methods Appl. Fluores.*, 2017, **5**, 012003.
18 Z. Han, X. Zhang, L. Qiao, C. Li, L. Jian, G. Shen and R. Yu, Efficient Fluorescence Resonance Energy Transfer-Based Ratiometric Fluorescent Cellular Imaging Probe for Zn^{2+} Using a Rhodamine Spirolactam as a Trigger. *Anal. Chem.*, 2010, **82**, 3108-3113.
19 X. Chen, F. Wang, J. Y. Hyun, T. Wei, J. Qiang, X. Ren, I. Shin and J. Yoon, Recent progress in the development of fluorescent, luminescent and colorimetric probes for detection of reactive oxygen and nitrogen species. *Chem. Soc. Rev.,* 2016, **45** (10), 2976-3016.
20 V. S. Lin, W. Chen, M. Xian and C. J. Chang, Chemical probes for molecular imaging and detection of hydrogen sulfide and reactive sulfur species in biological systems. *Chem. Soc. Rev.,* 2015, **44** (14), 4596-4618.
21 Y. Takano, K. Shimamoto and K. Hanaoka, Chemical tools for the study of hydrogen sulfide (H_2S) and sulfane sulfur and their applications to biological studies. *J. Clin. Biochem. Nutr.* 2016, **58** (1), 7-15.
22 G. Mao, T. Wei, X. Wang, S. Huan, D. Lu, J. Zhang, X. Zhang, W. Tan, G. Shen and R. Yu, High-Sensitivity Naphthalene-Based Two-Photon Fluorescent Probe Suitable for Direct Bioimaging of H_2S in Living Cells. *Anal. Chem.*, 2013, **85**, 7875-7881.
23 Y. Takano, K. Hanaoka, K. Shimamoto, R. Miyamoto, T. Komatsu, T. Ueno, T. Terai, H. Kimura, T. Nagano and Y. Urano, Development of a reversible fluorescent probe for reactive sulfur species, sulfane sulfur, and its biological application. *Chem. Commun.,* 2017, **53** (6), 1064-1067.
24 M. Ikeda, Y. Ishima, A. Shibata, V. T. G. Chuang, T. Sawa, H. Ihara, H. Watanabe, M. Xian, Y. Ouchi, T. Shimizu, H. Ando, M. Ukawa, T. Ishida, T. Akaike, M. Otagiri and T. Maruyama, Quantitative determination of polysulfide in albumins, plasma proteins and biological fluid samples using a novel combined assays approach. *Anal. Chim. Acta.,* 2017, **969**, 18-25.
25 W. Chen, C. Liu, B. Peng, Y. Zhao, A. Pacheco and M. Xian, New fluorescent probes for sulfane sulfurs and the application in bioimaging. *Chem. Sci.,* 2013, **4** (7), 2892-2896.
26 X. Han, X. Song, B. Li, F. Yu and L. Chen, A near-infrared fluorescent probe for sensitive detection and imaging of sulfane sulfur in living cells and in vivo. *Biomater. Sci.,* 2018, **6** (3), 672-682.
27 M. Gao, R. Wang, F. Yu, J. You and L. Chen, Imaging and evaluation of sulfane sulfur in acute brain ischemia using a mitochondria-targeted near-infrared fluorescent probe. *J. Mater. Chem. B,* 2018.
28 F. Yu, M. Gao, M. Li and L. Chen, A dual response near-infrared fluorescent probe for hydrogen polysulfides and superoxide anion detection in cells and in vivo. *Biomaterials,* 2015, **63**, 93-101.
29 M. Gao, F. Yu, H. Chen and L. Chen, Near-infrared fluorescent probe for imaging mitochondrial hydrogen polysulfides in living cells and in vivo. *Anal. Chem.,* 2015, **87** (7), 3631-3638.
30 W. Chen, E. W. Rosser, T. Matsunaga, A. Pacheco, T. Akaike and M. Xian, The Development of fluorescent probes for visualizing intracellular hydrogen polysulfides. *Angew. Chem. Int. Edit.,* 2015, **54** (47), 13961-13965.
31 W. Chen, E. W. Rosser, D. Zhang, W. Shi, Y. Li, W. J. Dong, H. Ma, D. Hu and M. Xian, A specific nucleophilic ring-opening reaction of aziridines as a unique platform for the construction of hydrogen polysulfides sensors. *Org. Lett.,* 2015, **17** (11), 2776-2779.
32 M. Gao, R. Wang, F. Yu, J. You and L. Chen, A near-infrared fluorescent probe for the detection of hydrogen polysulfides biosynthetic pathways in living cells and in vivo. *Analyst* 2015, **140** (11), 3766-3772.
33 Y. Huang, F. Yu, J. Wang and L. Chen, Near-infrared fluorescence probe for in situ detection of superoxide anion and hydrogen polysulfides in mitochondrial oxidative stress. *Anal. Chem.,* 2016, **88** (7), 4122-4129.
34 L. Zeng, S. Chen, T. Xia, W. Hu, C. Li and Z. Liu, Two-photon fluorescent probe for detection of exogenous and endogenous hydrogen persulfide and polysulfide in living organisms. *Anal. Chem.,* 2015, **87** (5), 3004-3010.
35 C. Liu, W. Chen, W. Shi, B. Peng, Y. Zhao, H. Ma and M. Xian, Rational design and bioimaging applications of highly selective fluorescence probes for hydrogen polysulfides. *J Am. Chem. Soc.,* 2014, **136** (20), 7257-7260.
36 W. Chen, A. Pacheco, Y. Takano, J. J. Day, K. Hanaoka and M. Xian, A single fluorescent probe to visualize hydrogen sulfide and hydrogen polysulfides with different fluorescence signals. *Angew. Chem. Int. Edit.,* 2016, **55** (34), 9993-9996.
37 H. Shang, H. Chen, Y. Tang, R. Guo and W. Lin, Construction of a two-photon fluorescent turn-on probe for hydrogen persulfide and polysulfide and its bioimaging application in living mice. *Sensor. Actuator. B-Chem.,* 2016, **230**, 773-778.
38 Q. Han, Z. Mou, H. Wang, X. Tang, Z. Dong, L. Wang, X. Dong and W. Liu, Highly selective and sensitive one- and two-photon ratiometric fluorescent probe for intracellular hydrogen polysulfide sensing. *Anal. Chem.,* 2016, **88** (14), 7206-7212.
39 X. Han, F. Yu, X. Song and L. Chen, Quantification of cysteine hydropersulfide with a ratiometric near-infrared fluorescent probe based on selenium-sulfur exchange reaction. *Chem. Sci.,* 2016, **7** (8), 5098-5107.
40 S. A. Hilderbrand and R. Weissleder, Near-infrared fluorescence: application to in vivo molecular imaging. *Curr. Opin. Chem. Biol.,* 2010, **14** (1), 71-79.
41 J. V. Frangioni, In vivo near-infrared fluorescence imaging. *Curr. Opin. Chem. Biol.,* 2003, **7** (5), 626-634.
42 H. Zhang, J. Liu, L. Wang, M. Sun, X. Yan, J. Wang, J. P. Guo and W. Guo, Amino-Si-rhodamines: A new class of two-photon fluorescent dyes with intrinsic targeting ability for lysosomes. *Biomaterials,* 2018, **158**, 10-22.
43 Y. Q. Sun, J. Liu, H. Zhang, Y. Huo, X. Lv, Y. Shi and W. Guo, A mitochondria-targetable fluorescent probe for dual-channel no imaging assisted by intracellular cysteine and glutathione. *J. Am. Chem. Soc.,* 2014, **136** (36), 12520-12523.

View Article Online
DOI: 10.1039/C8TB01794H

44 N. Boens, V. Leen and W. Dehaen, Fluorescent indicators based on BODIPY. *Chem. Soc. Rev.,* 2012, **41** (3), 1130-1172.
45 M. Gao, R. Wang, F. Yu and L. Chen, Evaluation of sulfane sulfur bioeffects via a mitochondria-targeting selenium-containing near-infrared fluorescent probe. *Biomaterials,* 2018, **160**, 1-14.
46 T. Ida, T. Sawa, H. Ihara, Y. Tsuchiya, Y. Watanabe, Y. Kumagai, M. Suematsu, H. Motohashi, S. Fujii, T. Matsunaga, M. Yamamoto, K. Ono, N. O. Devarie-Baez, M. Xian, J. M. Fukuto and T. Akaike, Reactive cysteine persulfides and S-polythiolation regulate oxidative stress and redox signaling. *Proc. Natl. Acad. Sci. USA,* 2014, **111** (21), 7606-7611.
47 H. Jurkowska, W. Placha, N. Nagahara and M. Wróbel, The expression and activity of cystathionine-γ-lyase and 3-mercaptopyruvate sulfurtransferase in human neoplastic cell lines. *Amino Acids,* 2011, **41** (1), 151-158.
48 H. Jurkowska and M. Wróbel, N-acetyl-L-cysteine as a source of sulfane sulfur in astrocytoma and astrocyte cultures: correlations with cell proliferation. *Amino Acids,* 2008, **34** (2), 231-237.
49 V. S. Lin, A. R. Lippert and C. J. Chang, Cell-trappable fluorescent probes for endogenous hydrogen sulfide signaling and imaging H_2O_2-dependent H_2S production. *Proc. Natl. Acad. Sci. USA,* 2013, **110** (18), 7131-7135.
50 M. Iciek and L. Wlodek, Biosynthesis and biological properties of compounds containing highly reactive, reduced sulfane sulfur. *Pol. J. Pharmacol.,* 2001, **53** (3), 215-225.
51 J. I. Toohey, Persulfide sulfur is a growth-factor for cells defective in sulfur metabolism. *Biochem. Cell Biol.,* 1986, **64** (8), 758-765.
52 L. Y. Sheen, H. W. Chen, Y. L. Kung, C. T. Liu and C. K. Lii, Effects of garlic oil and its organosulfur compounds on the activities of hepatic drug-metabolizing and antioxidant enzymes in rats fed high- and low-fat diets. *Nutr. Cancer,* 1999, **35** (2), 160-166.
53 C. Roffe, Hypoxia and stroke. *Age Ageing,* 2002, **31**, 10-13.
54 C. Peers, H. A. Pearson and J. P. Boyle, Hypoxia and Alzheimer's disease. *Essays Biochem.,* 2007, **43**, 153-164.
55 X. Y. Zhu, S. J. Liu, Y. J. Liu, S. Wang and X. Ni, Glucocorticoids suppress cystathionine gamma-lyase expression and H_2S production in lipopolysaccharide-treated macrophages. *Cell. Mol. Life Sci.,* 2010, **67** (7), 1119-1132.

View Article Online
DOI: 10.1039/C8TB01794H

Table of Contents

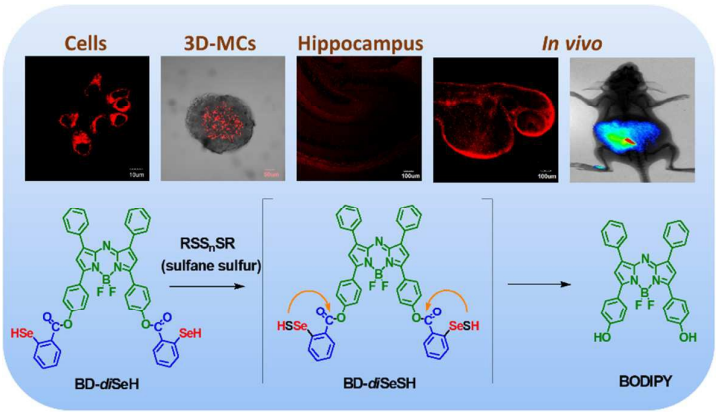

Imaging of sulfane sulfur expression changes in living cells, in 3D-multicellular spheroid, in hippocampus and *in vivo* under hypoxia stress via a selenium-containing near-infrared fluorescent probe.